CHEMICAL ENGINEERING TRANSACTIONS Volume 18, 2009
Editor Jiří Klemeš
 ISBN 978-88-95608-04-4 ISSN 1974-9791
DOI: 10.3303/CET0918145

A switching pressure approach in simulation and optimization of a reverse osmosis unit

Cristiano Cerrato[1], Andrea Pietro Reverberi[2,*] , Vincenzo Dovì[2] and Agostino Giacinto Bruzzone[3]

[1]DIMSET - Department of Machinery, Energy Systems and Transports, via Montallegro 1 - 16145 Genova (ITALY).
[2]DIChePP - Department of Chemical Engineering and Process, via Opera Pia 15 - 16145 Genova (ITALY).
[3]DIPTEM - Department of Production Engineering, Thermoenergetics and Mathematical Modelling, via Opera Pia 15 - 16145 Genova (ITALY).
reverb@dichep.unige.it

1. Introduction

Water purification is nowadays one of the most challenging topic both from an applicational and theoretical point of view.
Membrane lifetime and permeate flux are mainly conditioned by fouling and concentration polarization that, though acting on two different time scales, may drastically reduce the yield of the global process [1-5]. The most interesting approach to better foresee the concentration trend near the membrane surface is based on an unsteady-state modelling of the diffusion-convection equation in one or two space variables [6-8]. In this paper, we propose a numerical simulation of a single-step separation in a spiral wound module in unsteady-state regime with axial and radial diffusion. The scheme is organized as follows. In section 2, we outline the essentials of the model and we describe the numerical algorithm. In section 3, we present the results of the simulations obtained with different values of the parameters conditioning the yield of the global process. Besides, we study the effects of a pulsating regime of pressure on the permeate flux for different switching times. Finally, we draw the conclusion and trace the direction for future works.

2. The model

In Fig.1 , a fluid containing a dissolved salt enters a region between two membranes. The membranes are supported by spacers, represented by filaments arranged in configurations according to various constructive schemes; in particular, cavity, zigzag or submerged sequences of spacers have been experimentally proposed to improve the yield of the global process reducing the effect of concentration polarization. In this case, we assume that they are equally spaced along the x-direction. For symmetry considerations, the coordinate system is placed on the symmetry axis at inlet of a channel of length L and half-height h.

Please cite this article as: Cerrato C., Reverberi A., Dovi V. and Bruzzone A., (2009), A switching pressure approach in simulation and optimization of a reverse osmosis unit, Chemical Engineering Transactions, 18, 887-892 DOI: 10.3303/CET0918145

The convection-diffusion equation of a chemical species present in the solution between two parallel membranes can be written as:

$$\frac{\partial c}{\partial t} = \frac{\partial}{\partial y}\left(D_y \frac{\partial c}{\partial y} \right) + \frac{\partial}{\partial x}\left(D_x \frac{\partial c}{\partial x} \right) - u\frac{\partial c}{\partial x} - v\frac{\partial c}{\partial y} \tag{1}$$

where c is the concentration of the solute, D_x and D_y the axial and radial diffusivities, u and v the axial and radial velocities, t is the time and x,y the axial and radial coordinates as indicated in Fig.1.

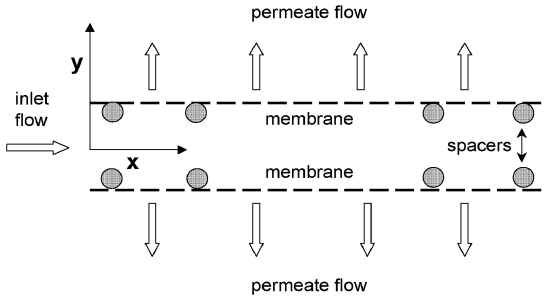

Fig.1 - Sketch of a membrane channel with spacers according to the discretization scheme adopted in this work.

The axial velocity profile at the channel inlet is typical of a fully developed motion according to a Poiseuille parabolic law.
We define the following dimensionless variables:

$C=c/c_0$, $X=x/L$, $Y=y/h$, $U=u/u_0$, $V=vL/u_0h$; $D_Y=D_yL/u_0h^2$; $D_X=D_x/u_0L$ (2)

that are replaced into expression (1) to obtain the form:

$$\frac{\partial C}{\partial T} = \frac{\partial}{\partial Y}\left(D_Y \frac{\partial C}{\partial Y} \right) + \frac{\partial}{\partial X}\left(D_X \frac{\partial C}{\partial X} \right) - U\frac{\partial C}{\partial X} - V\frac{\partial C}{\partial Y} \tag{3}$$

The velocity profiles U and V present in the previous equation are not modelled according to the well-known Navier-Stokes equation, but two ad-hoc expressions for spiral wound membranes are adopted, that is:

$$U(X,Y) = \frac{1}{u_0}\frac{dP}{dx}\frac{h^2}{\eta m^2}\left(1 - \frac{v_W x}{u_0 h}\right)\left\{(m+1)ln\left[m\left(1-\frac{y}{h}\right)+1\right] - m\left(1-\frac{y}{h}\right)\right\} \tag{4}$$

$$V(X,Y) = 0.5\frac{v_W yL}{u_0 h^2}\left[3 - \left(\frac{y}{h}\right)^2\right] - \frac{v_W^2 L}{280\nu u_0}\left[2 - 3\left(\frac{y}{h^2}\right) + \left(\frac{y}{h}\right)^6\right] \tag{5}$$

The constant m is a tuning parameter taking into account the curved geometry of the apparatus, the presence of spacers, their thickness and density in the cavity between membranes [9].
The velocity expressions here reported depend both on the spatial coordinates and on the wall permeation velocity v_W through Eqs. (4) and (5). In its turn, the wall permeation velocity is related to the wall concentration, as it will be discussed later. Therefore, the coefficients of the first order derivatives in Eq.(3) are function of the

boundary values of the dependent variable at Y=1. We recall now briefly some features of the discretization scheme here adopted, which is traditionally explicit as far as Eq.(3) is concerned but it contains some implicit features when it is applied to the boundary conditions.

Assuming that $h_1 = \Delta X$, $h_2 = \Delta Y$ and $k = \Delta T$ as discretization intervals for space and time variables respectively, we use first order forward expressions for all derivatives present in Eq.(2) to obtain:

$$C_{i,j}^{n+1} = \left(\frac{k}{h_1}U_{i,j}^n + \frac{D_X k}{h_1^2}\right)C_{i-1,j}^n + \left(\frac{k}{h_1}U_{i,j}^n + \frac{k}{h_2}V_{i,j}^n + \frac{2D_X k}{h_1^2} + \frac{2D_Y k}{h_2^2} - 1\right)C_{i,j}^n + \frac{D_X k}{h_1^2}C_{i+1,j}^n + \left(\frac{k}{h_2}V_{i,j}^n + \frac{D_Y k}{h_2^2}\right)C_{i,j-1}^n + \frac{D_Y k}{h_2^2}C_{i,j+1}^n \qquad (6)$$

where $C^n_{i,j}$ indicates the concentration value of a generic point at ($i\Delta X$; $j\Delta Y$) coordinates at the n-th time interval, with 1<i<imax and 1<j<jmax. Eq.(6) represents the so-called computational molecule for the concentration updating of a 2-d parabolic equation at inner points of the space grid.

At the start, the unit is filled with a solution at a concentration equal to the one of the cell feed. So, the initial condition is:

$$C(0,X,Y) = 1 \qquad (7)$$

The boundary conditions are :

$$C(T,0,Y) = 1 \qquad (8)$$

$$\left.\frac{\partial C}{\partial X}\right|_{i\,max,j}^{n} = \left.\frac{\partial C}{\partial X}\right|_{i\,max-1,j}^{n} \Rightarrow \frac{\partial^2 C}{\partial X^2}(T,1,Y) = 0 \qquad 9)$$

$$\frac{\partial C}{\partial Y}(T,X,0) = 0 \qquad (10)$$

The boundary condition at the membrane surface requires a more careful attention. A balance between diffusive and convective mass transport can be written as:

$$D_Y \frac{\partial C}{\partial Y}(T,X,1) = V_W\left(C_W - C_P\right) = V_W C_W R \qquad (11)$$

In Eq.(11), it is assumed that the permeate concentration C_P depends of the wall concentration C_W according to an expression containing the rejection factor R, namely:

$$C_P = C_W(1-R) \qquad (12)$$

The membrane permeation velocity at the wall V_W can be described by the following phenomenological relation [6]:

$$V_W(X,T) = v_W L/u_0 h = A(\Delta P - \Delta\Pi)L/u_0 h \qquad (13)$$

where ΔP is the pressure gap at fixed X between two membrane sides and A is the membrane permeability. Besides, the difference of osmotic pressure $\Delta\Pi$ is described as a linear function of the membrane concentration at the wall:

$$\Delta\Pi = K_0(C_W - C_P) = K_0 C_W R \qquad (14)$$

where K_0 is the osmotic pressure constant.

Replacing Eqs. (13)-(14) into Eq.(11) and writing in terms of finite differences, we get:

$$\left(\frac{AR^2 LK_0 c_0}{u_0 h}\right)(C_{i,j\,max}^n)^2 + \left(\frac{D_Y}{h_2} - \frac{ARL}{u_0 h}(P_0 - \lambda LX)\right)C_{i,j\,max}^n - \frac{D_Y}{h_2}C_{i,j\,max-1}^n = 0 \qquad 15)$$

where λ is the head loss per unit lenght of the membrane, P_0 is the inlet pressure and $P = P_0 - \lambda LX$ is the inner fluid pressure in a generic point located at (iΔX; jΔY)

coordinates. The concentration at the permeable wall can be calculated without iteration by simply solving the previous algebraic equation for each point belonging to the membrane, provided the concentration values in the points $C^{n}_{i,jmax-1}$ close to the membrane have been previously calculated from (6).
We have linearly interpolated the experimental data taken from Tay et al.[10] and we have obtained a semi-empirical correlation between pressure and permeability that reads:

$$A=(1.9\cdot10^{4}\ P+1.38\cdot10^{11})^{-1} \qquad (16)$$

Finally, the global problem can be defined by joint use of Eqs. (3) and Eqs.(7-16).
The effects of concentration on viscosity and diffusivity have been neglected, as we focus our attention on sodium chloride in water whose diffusivity variation is less than 5% in the range [0.125-1.5] normality.

3. Results and discussion

The combined effects of pressure and concentrate flow rate on the yield of the process are visualized in Fig.2, where the curves are loci of points at constant permeate flux.

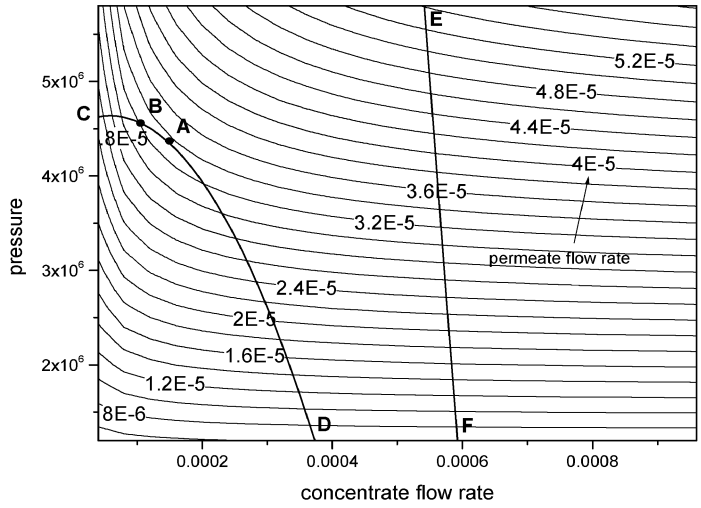

Fig.2 - Contour plot of permeate flux versus the concentrate flow rate and operating pressure. Curve CD: scheme of a centrifugal pump characteristic curve. Curve EF: scheme of a reciprocating pump characteristic curve.

These lines tend to become parallel and horizontal in the right part of the contour plot, namely for high values of solution flow rate. This fact can be explained remembering that the beneficial effects of a high pressure on permeate flux are prevailing on polarization, provided the velocity U is high enough to reduce the width of the saturation zone whatever the pressure. On the contrary, the left part of the plot is covered by steeper lines, which are getting more and more vertical for high pressure values, suggesting that the role of pressure is almost uninfluential if there is no "cleaning" effect of velocity on polarization.

Besides, this diagram can be useful to optimize the permeate flow by superposing the characteristic curves of a pump on the aforementioned lines of constant permeate flux. This is possible provided the flow rate of the pump is rescaled with respect to the flow rate of a single reverse osmosis channel. In case of a reciprocating pump, the characteristic curve is an almost vertical line and the optimum matching point lies at the highest operating pressure. In case of a centrifugal pump, remembering that its characteristic curve has a typically bended shape, a point B corresponding to a high pressure on this line does not necessarily correspond to the optimum point of highest permeate flux, here represented by the point A in Fig.2.

Kennedy *et al.* [11] were the first who carried out a theoretical explanation on why a pulsed velocity in reverse osmosis unit should have a beneficial action on the wall mass transfer coefficient. In their study, the ratio γ between the mass transfer coefficient in a square-wave pulsating flow and the same coefficient in a steady-state flow was expressed as:

$$\gamma = 0.5\,|1+k_1 f\,|^p + 0.5\,|1-k_1 f\,|^p = G(f) \tag{17}$$

where k_1 is a coefficient depending on the geometry of the channel and on the average velocity of flow, f is the frequency of the disturbance and p is an exponent varying in the range [0.33-0.8] for growing values of the Reynolds number.

A simple scheme of desalination plant at pilot scale is described by Al-Bastaki *et al.* [12], where a pulsating regime was realized by periodically switching the valve on the concentrate flux at the exit of the reverse osmosis cell. We will assume in the following that the diffusivity D_Y in Eq.(11), concerning the boundary condition at the permeable wall, is dependent of the frequency of pressure according to the same power law described by Eq.(17), namely:

$$\gamma = \frac{D_Y}{D_{Y,s}} = G(f) \tag{18}$$

where $D_{Y,s}$ is the unperturbed value of diffusivity.

In Fig.3, the permeate flux is plotted versus time in case of a pressure cyclic forcing applied after a short initial stabilization time according to our simulation model. We assume a ± 1MPa square wave symmetric perturbation around an average value of 3 MPa. To make a comparison, the curve corresponding to a constant pressure feed is superposed. The area between each curve and the horizontal axis gives the total mass of permeate resulting at the end of the process. In this case, we calculated a 2.7% increase of the total permeate mass in case of two complete operating cycles, a result which is consistent with the aforementioned findings.

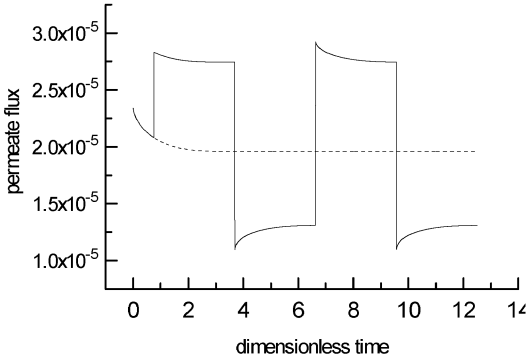

Fig.3 - Plot of permeate flux versus time in case of constant feed (dashed line) and during a pulsed pressure feed (solid line) for $P=3\pm1\cdot10^6$ *and* $c_0=10$.

4. Conclusions

In this study, we have proposed a simulation model of an unsteady-state single stage reverse osmosis process in two space variables. A semi-empirical correlation between pressure and permeability has been adopted, together with a power law correlation between the wall diffusivity and the number of pressure pulsations during the operating cycle. The role of the parameters governing the process has been discussed with respect to the permeate flux according to the effects of polarization.

References

[1] Kim YM, Kim SJ, Kim YS, Lee S, Kim In S, Kim Joon H. Desalination 2009; 238 (1-3): 312.

[2] Vishnu G, Palanisami S, Joseph K. Journal of Cleaner Production 2008; 16 (10): 1081-1089.

[3] Jeppesen T, Shu L, Keir G, Jegatheesan V. Journal of Cleaner Production 2008; 17 (7): 703.

[4] Goosen MFA, Sablani SS, Al-Hinai H, Al-Obeidani S, Al-Belushi R, Jackson D. Separation Science and Technology 2004; 39 (10): 2261-2297.

[5] Hoek EMV, Allred J, Knoell T, Jeong B-H. Journal of Membrane Science 2008; 314: 33.

[6] S. Kim, E.M.V. Hoek, Desalination 186 (2005), 111-128.

[7] A.L. Ahmad, M.F. Chong, S. Bhatia, Chemical Engineering Journal 132 (2007) 183-193.

[8] K. Madireddi, R.B. Babcock, B. Levine, J.H. Kim, M.K. Stenstrom, Journal of Membrane Science 157 (1999),13-34.

[9] D. Bhattacharyya, S.L. Back, R.I. Kermode, Journal of Membrane Science 48 (1990), 231-262.

[10] Tay KG, Song L, Ong SL , Ng WJ. Journal of Environmental Engineering 2005; 131 (11): 1481-1487.

[11] Kennedy TJ, Merson RL, McCoy BJ. Chemical Engineering Science 1974; 29:1927-1931.

[12] Al-Bastaki NM, Abbas A. Separation Science and Technology 1998; 33 (16): 2531-2540.